

## Slow dynamics and aging in colloidal gels studied by x-ray photon correlation spectroscopy

Andrei Fluerașu,<sup>1</sup> Abdellatif Moussaïd,<sup>1</sup> Anders Madsen,<sup>1</sup> and Andrew Schofield<sup>2</sup>

<sup>1</sup>European Synchrotron Radiation Facility, Boîte Postale 220, F-38043 Grenoble, France

<sup>2</sup>Department of Physics and Astronomy, University of Edinburgh, Edinburgh, United Kingdom

(Received 13 November 2006; revised manuscript received 22 March 2007; published 2 July 2007)

Slow, nonequilibrium dynamics during delayed sedimentation in a colloidal depletion gel was studied by x-ray photon correlation spectroscopy. The intermediate scattering functions change during the process from stretched to compressed exponential decays, indicating a jamming transition toward full aging. A complex aging behavior follows this process; it is proposed that large-scale network deformations trigger an unjamming, leading to the final collapse of the gel.

DOI: 10.1103/PhysRevE.76.010401

PACS number(s): 83.80.Kn, 61.10.Eq, 82.70.Dd

Aggregation and gelation are topics of fundamental interest in condensed-matter physics [1] that also have many direct industrial applications. Delayed sedimentation in transient gels is a nonequilibrium phenomenon encountered in a variety of soft-matter systems, including colloidal suspensions with strong enough short-ranged attractive interactions. Due to the interactions, the colloidal particles can aggregate at much lower concentrations (e.g., 20%) than those leading to the formation of glasses in hard-sphere systems ( $\approx 60\%$ ), forming a space-filling structure often denoted a gel. However, this nonequilibrium structure slowly evolves, until the spatial connectivity is lost and the gel suddenly collapses. The formation and collapse of transient gels have been addressed recently by experimental [2–6] and theoretical [7,8] work. However, despite the interest, the aging behavior and mechanisms that govern the final collapse of the gel remain uncertain.

A common generic behavior of disordered soft-matter systems, such as colloidal gels, is the presence of several dynamical relaxation mechanisms. The fast(er) ones correspond to the confined motion of individual particles or aggregates in cages or clusters created by neighboring particles or aggregates. Because the clustering can lead to structural arrest, such systems are generally nonergodic. It is through the slow relaxations, corresponding to structural rearrangements equivalent to the  $\alpha$  process in glasses, that the system eventually can reach equilibrium and ergodicity may be restored. The fast relaxation modes and the transition to nonergodicity have received a considerable amount of attention. Theoretical studies based on mode coupling theory [1,7], numerical simulations [8,9], and experimental studies based mainly on dynamic light scattering [10] and neutron scattering techniques agree on a few general points: (i) the fast dynamics modes are arrested and the correlation functions terminate in a  $Q$ -dependent plateau; (ii) the fast relaxation modes are *diffusive* or *subdiffusive*, i.e., the relaxation rates  $\Gamma$  scale as  $\Gamma \propto Q^n$  with  $n \geq 2$ , and the intermediate scattering functions (ISFs) are well described by the Kohlrausch form  $g_1 \propto \exp[-(\Gamma t)^\gamma]$ , with exponent  $\gamma \leq 1$ ; and (iii) the relaxation rates  $\Gamma$  do not change in time (i.e., no aging is observed).

In contrast with the studies on the fast dynamics, there have been only a few experiments probing the slow relaxation modes in gels and other “glassy” systems (see, for instance, Refs. [11–13]). These studies, as well as theoretical

investigations [14] and numerical simulations [15], seem to agree on some general points: (i) often the ergodicity is restored by these slow relaxations; (ii) the dynamics is *hyperdiffusive*, i.e., the relaxation rates scale as  $\Gamma \propto Q^n$  with  $n \leq 2$ , and the ISFs follow  $g_1 \propto \exp[-(\Gamma t)^\gamma]$ , with  $\gamma \geq 1$ ; (iii) the relaxation rates change in time (aging).

In this Rapid Communication, we study the slow dynamics in a colloidal transient gel by x-ray photon correlation spectroscopy (XPCS). The sample, a mixture of sterically stabilized polymethylmethacrylate (PMMA) particles and non adsorbing random-coil polystyrene (PS) dispersed in cis-decalin, is a well-characterized transient gel (in terms of its phase diagram) [1,16]. The addition of nonadsorbing polymers (radius of gyration  $r_g$ ) to the suspension of hard-sphere colloids causes an effective attraction of range  $\approx 2r_g$  between particles via the depletion mechanism [1]. The attraction leads to a diverse phase behavior, and a variety of nonequilibrium aggregates have been observed at high polymer concentrations. The equilibrium phase diagram depends on the ratio  $\xi = r_g/R$ , and on the colloid and polymer concentrations. Here, the radius of the PMMA particles is  $R \approx 111.6$  nm (with a size polydispersity of 7%), and  $\xi = 0.11$ . The colloid volume fraction is  $\Phi = 0.2$ , and the polymer concentration is the overlap concentration  $c_p = c^* = 4.3$  mg/cm<sup>3</sup>. The phase diagram of the PMMA-PS mixtures has been carefully characterized [3,16], and, as prepared, the system is far into the transient gel phase region. Once the solutions are prepared, they are left tumbling in a large cell. Before starting the experiment, the sample is filled into a 1.5 mm quartz capillary (this is always considered as the time origin,  $t_a = 0$ , i.e., age zero), which then is sealed to prevent evaporation. The XPCS experiments were performed using partially coherent x rays at the ID10A beamline (Troika) of the European Synchrotron Radiation Facility. A single-bounce Si(111) crystal monochromator was used to select 8 keV x rays, having a relative bandwidth of  $\Delta\lambda/\lambda \approx 10^{-4}$ . A Si mirror downstream of the monochromator suppressed higher-order light. A transversely coherent beam was defined by slit blades with highly polished cylindrical edges. The slit size was varied between 5 and 20  $\mu\text{m}$  in the vertical and horizontal directions. Under these conditions, the (partially) coherent x-ray flux was  $\sim 10^9$  photons/s. The scattering from the PMMA-PS gels was recorded by a charge-coupled device (CCD) with 22  $\mu\text{m}$  pixels located 2.3 m downstream of the sample. The CCD

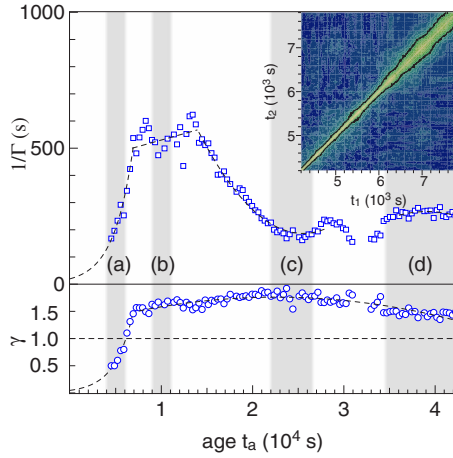


FIG. 1. (Color online) Correlation times  $1/\Gamma$  and exponents  $\gamma$  as a function of age obtained from equal-age slice fits of the two-time correlation functions calculated for  $QR=3$ . The gray areas highlight the time intervals defined in the text as “early” (a), “full aging” (b), “intermediate” (c), and “late” (d) stages (dashed lines are guides for the eyes). Inset: Contour plot of the two-time correlations [Eq. (1)] showing here the transition to full aging. The black lines show a level corresponding to the full width at half maximum of the correlation functions.

was used in photon-counting mode under direct illumination conditions, which enables multispeckle XPCS. Series of speckle patterns were recorded with an exposure time of 1 s at a frame repetition rate of 0.15 Hz. The nonequilibrium and nonstationary dynamic properties were investigated using two-time correlation functions [17],

$$C(Q, t_1, t_1) = \frac{\langle I(Q, t_1)I(Q, t_2) \rangle_{\text{pix}}}{\langle I(Q, t_1) \rangle_{\text{pix}} \langle I(Q, t_2) \rangle_{\text{pix}}}. \quad (1)$$

Here, the ensemble averages are performed over many pixels of the CCD detector, all having the same  $Q$  value. The natural variables to describe the two-time correlation functions (see inset in Fig. 1) are the average time or age  $t_a = (t_1 + t_2)/2$ , measured by the distance along the  $t_1 = t_2$  diagonal, and the time difference  $t = |t_1 - t_2|$ , which is the distance from the  $t_1 = t_2$  diagonal in the perpendicular direction. In an equilibrium system, the two-time correlation functions depend only on the time difference  $t$ , and hence the two-time correlation contour lines are parallel. In such a situation the usual one-time correlation function is retrieved by averaging the two-time correlation function over different ages. For limited age intervals, when the two-time correlations point toward a quasistationary state of the system, the one-time intensity autocorrelation functions

$$g_2(Q, t) = \frac{\langle \langle I(Q, t_0)I(Q, t_0 + t) \rangle_{t_0} \rangle_{\text{pix}}}{\langle \langle I(Q, t_0) \rangle_{t_0}^2 \rangle_{\text{pix}}} \quad (2)$$

were calculated by using a standard multiple- $\tau$  algorithm [18]. All time-averaged correlation functions are calculated for individual pixels and subsequently averaged over coarse-grained rings of pixels on similar  $Q$  values. Assuming a Gaussian distribution of the temporal fluctuations at a fixed

$Q$ , the ISFs  $g_1(Q, t)$  were calculated from the correlation functions using the Siegert relationship  $g_2 = 1 + \beta g_1^2$ , where  $\beta$  is the speckle contrast (in this setup around 20%). XPCS data were recorded during the delayed sedimentation process of the PMMA-PS transient gel for a total duration of about 9 h, starting at  $t_a = 4200$  s after the sample preparation. The two-time correlation functions (Fig. 1, inset) reveal a complex time evolution of the dynamic properties of the gel. To extract the age behavior of the relaxation rate  $\Gamma$  and the exponent  $\gamma$ , the two-time correlation functions were averaged over  $\approx 5$ -min-wide equal-age slices and fitted with a Kohlrausch form,  $g_1(Q, t) = \exp[-(\Gamma t)^\gamma] + g_\infty$ . In all measurements the ergodicity was fully restored by these slow relaxations, i.e., the nonergodicity parameter  $g_\infty$  was found to be 0. The time evolution of the correlation time  $\tau = 1/\Gamma$  can be seen in Fig. 1. After an initial stage ( $t_a \leq 7000$  s) during which the correlation times increase exponentially with age, a region with huge fluctuations is entered. We attribute these strong fluctuations to large-scale rearrangements in the gel. Such behavior has been observed previously in different systems, and a universal model for aging in soft matter was proposed [11,12]. However, strong deviations from this picture occur around  $t_a \approx 1.4 \times 10^4$  s, when the correlation times start decreasing before reaching a plateau around  $t_a \approx 2.2 \times 10^4$  s. Some temporary, but pronounced, decay in the correlation times follows around  $t_a \approx 3 \times 10^4$  s. Like those occurring earlier, these fluctuations probably indicate the breaking and rearrangement of some large-scale spatial inhomogeneities. A final plateau is reached around  $t_a \geq 3.5 \times 10^4$  s. At the end of the experiment, visual inspection confirmed that the gel had started collapsing, but the sedimentation interface was still above the probed volume. In Fig. 1 the age evolution of the Kohlrausch exponent is also shown, and a remarkable crossover from  $\gamma < 1$  to  $\gamma > 1$  is happening during the early stages of the process. In order to better characterize this process, and also to capture the  $Q$ -dependence in a more efficient way, a standard multiple- $\tau$  autocorrelation scheme and an analysis of the static scattering were performed for four different time intervals. The time intervals are highlighted by the gray areas in Fig. 1 and defined as (a) “early stages,” (b) “full aging stages,” (c) “intermediate stages,” and (d) “late stages” of the delayed sedimentation process. The results reported here are robust to small changes in these intervals. The time-average scattering profiles, shown in Fig. 2, confirm that the static properties of the gel do not change in time and, for instance, there is no indication of the forthcoming gel collapse in the data. The static data also confirm that the scattering comes from the PMMA spheres and decay following Porod behavior  $I \propto Q^{-4}$  (Fig. 2). The inset in Fig. 2 shows the structure factor, which has a characteristic peak at  $QR \approx 3.9$ , which is a signature of the presence of dense areas in the sample.

The ISFs, fitted to the Kohlrausch form, are shown in Fig. 3 for six different values of  $Q$  ranging from  $QR=3.6$  to 10.7, and for the four time intervals considered here. Plotted on a lin-log scale as a function of the reduced time  $\Gamma t$ , the intermediate scattering functions would appear as straight lines if the relaxations were purely exponential, i.e., if  $\gamma=1$ . From Fig. 3(a), it can be seen that the ISFs have a small positive curvature during the early stages of the process, which is

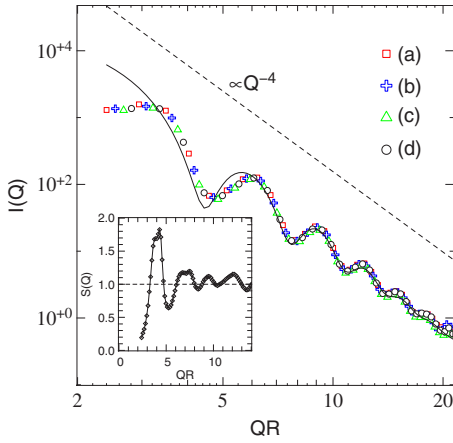


FIG. 2. (Color online) Small-angle x-ray scattering profiles during the delayed sedimentation process: (a) early stages, (b) full aging, (c) intermediate stages, and (d) late stages. The black line shows a fit for the form factor of polydisperse hard-sphere colloids with a Schulz particle size distribution. The deviation between data and model at low  $QR$  is due to the structure factor (shown in the inset) caused by interactions between the colloids. The dashed line is guide to the eye and has slope  $-4$ .

indicative of a stretched exponential shape ( $\gamma < 1$ ). In sharp contrast, during the intermediate and late stages, the curvatures of the ISFs become negative, which is an indication of compressed exponentials with  $\gamma > 1$ . Kohlrausch-type relaxations with  $\gamma > 1$  have been found in several different systems believed to be in jammed states [12,19–23], and hence our measurements may indicate a jamming transition occurring during the initial gel stages. While a temperature-induced transition from stretched to compressed exponential relaxations has been found in a lamellar sponge phase [24], this Rapid Communication reports, to our knowledge, the first signs of a jamming transition toward a fully aged state

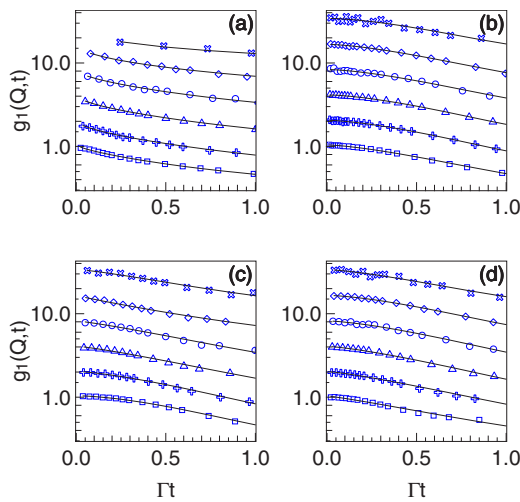


FIG. 3. (Color online) ISFs calculated for  $QR=3.6$  (squares), 5.0 (crosses), 6.5 (triangles), 7.9 (circles), 9.3 (diamonds), and 10.7 (stars), and for four different time intervals: (a) early, (b) full aging, (c) intermediate, and (d) late stages; for clarity the ISFs have been multiplied by 1, 2, 4, 8, 16, and 32.

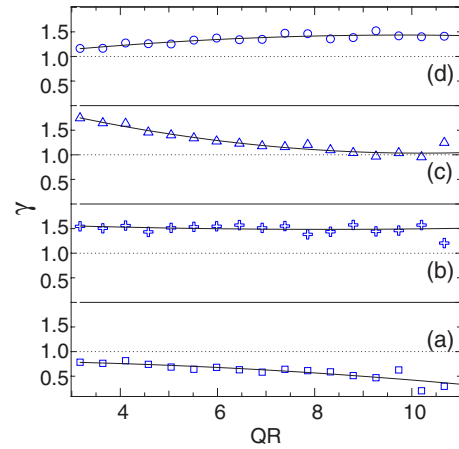


FIG. 4. (Color online) Kohlrausch exponent  $\gamma$  as a function of  $Q$  during the early (a), full aging (b), intermediate (c), and final (d) stages.

by a change in the Kohlrausch exponent  $\gamma$  from subunitary to supraunitary.

The age- and  $Q$ -dependent Kohlrausch exponents of the ISFs in the PMMA-PS gels can better be seen in Fig. 4. While at the early stages they are subunitary on all length scales, the picture changes in the full-aging regime, where the relaxations are better described by compressed exponentials on all length scales. However, an intriguing process starts developing during the intermediate stages [Fig. 4(c)], when the correlation functions are better described by exponential decays ( $\gamma \approx 1$ ) on small length scales ( $QR \sim 10$ ), but are still compressed exponentials on large length scales ( $QR \sim 3-4$ ). We associate this process, which could be called “unjamming” and can be explained by some small length-scale rearrangements of the network, with the increase in the diffusion starting around  $t_a = 1.4 \times 10^4$  s (see Fig. 1). However, this effect is not permanent, and the network seems to have healed at the late stages [Fig. 4(d)], when the Kohlrausch exponents  $\gamma$  are again larger than 1 on all length

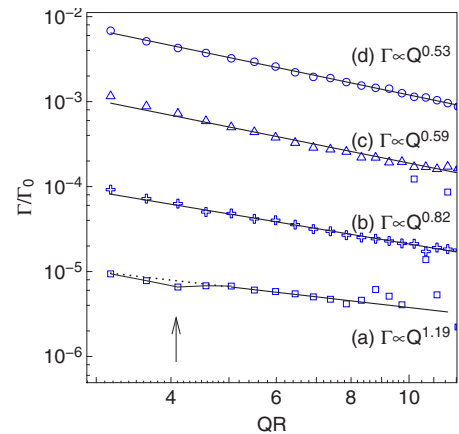


FIG. 5. (Color online) Reduced relaxation rate  $\Gamma/\Gamma_0$  as a function of  $Q$ , and fits with power laws  $\Gamma \propto Q^n$  for (a) early, (b) full aging, (c) intermediate, and (d) final stages. For clarity the curves have been multiplied by 1, 20, 100, and 1000, respectively.

scales. Interestingly, the data in Fig. 4 even seem to indicate that, at late stages, a similar unjamming process is initiated on large length scales, with a resulting decrease in  $\gamma$  and a positive slope of the curve in Fig. 4(d). A possible scenario would be that, when the transient gel has reached a certain age, the largest clusters start disaggregating, while the fragments and smaller clusters stay jammed.

The dispersion relations of the relaxation rates can be seen in Fig. 5. The reduced relaxation rate  $\Gamma/\Gamma_0$  is defined using the free diffusion coefficient  $D_0=k_B T/6\pi\eta R$  of the colloidal particles, and  $\Gamma_0=D_0Q^2$ . Here  $\eta=3.38$  cP is the kinematic viscosity of the solvent. The relaxation rates scale as  $\Gamma\propto Q^n$  with  $n<2$ , and point toward a hyperdiffusive character of the dynamics probed here. Interestingly, this is valid even at early times, when the ISFs are still best described by stretched exponential decays with  $\gamma<1$ . In Fig. 5, there are indications of a slowing down of the dynamics near the structure factor peak (arrow). This effect, known as de Gennes narrowing, can be seen only in the early stages [Fig. 5(a)], when the sample is closest to a liquid state, and vanishes in the intermediate and late stages of the process. This suggests that, in the jammed state, the dynamics is dominated by cooperative relaxations. Cipelletti *et al.* have stud-

ied aqueous colloidal polystyrene gels, and they explained the observed  $\gamma\sim 1.5$  and  $\Gamma\propto Q$  behavior by syneresis-induced network deformations [25]. This behavior mimics our results for the full-aging [Fig. 5(b)] regime, and hence we may speculate that large-scale deformations trigger the cluster disaggregation process and lead to the gel collapse. Indeed, for late stages [Fig. 4(d)], our results are close to those reported by Solomon *et al.* [26] ( $\Gamma\propto Q^{1/2}$ ), pointing toward cluster disaggregation as the main feature in the dynamics right before the collapse. This picture is also supported by the isotropy of the dynamical properties probed here. Indeed, the relaxation rates measured in the vertical or horizontal directions are the same in all the jammed states, indicating that gravity-induced shear effects are negligible, and that the dominant dynamical process is the release of the network-induced stresses. However, a subtle dynamic anisotropy effect can be seen in the more “fluidlike” states, during the early stages [Fig. 5(a)]. It is also clear that the capillary size is an important factor in these experiments. Unlike what happens in a large container, in a small capillary, adhesion between the gel and the inner wall of the cell may create a “partial collapse.” Further studies of these subtle flow and capillary size effects are planned for future experiments.

- 
- [1] K. N. Pham *et al.*, *Science* **296**, 104 (2002).  
 [2] M. L. Kilfoil, E. E. Pashkowski, J. A. Masters, and D. Weitz, *Philos. Trans. R. Soc. London, Ser. A* **361**, 753 (2003).  
 [3] W. C. K. Poon *et al.*, *Faraday Discuss.* **12**, 143 (1999).  
 [4] W. C. K. Poon, A. D. Pirie, M. D. Haw, and P. N. Pusey, *Physica A* **235**, 110 (1997).  
 [5] L. Starrs, W. C. K. Poon, D. J. Hibberd, and M. M. Robins, *J. Phys.: Condens. Matter* **14**, 2485 (2002).  
 [6] N. A. M. Verhaegh *et al.*, *Physica A* **242**, 104 (1997).  
 [7] J. Bergenholtz, M. Fuchs, and T. Voigtmann, *J. Phys.: Condens. Matter* **12**, 6575 (2000).  
 [8] M. D. Haw, M. Sievwright, W. C. K. Poon, and P. N. Pusey, *Adv. Colloid Interface Sci.* **62**, 1 (1995).  
 [9] K. Dawson, G. Foffi, M. Fuchs, W. Götze, F. Sciortino, M. Sperl, P. Tartaglia, Th. Voigtmann, and E. Zaccarelli, *Phys. Rev. E* **63**, 011401 (2000).  
 [10] A. H. Krall and D. A. Weitz, *Phys. Rev. Lett.* **80**, 778 (1998).  
 [11] M. Bellour, A. Knaebel, J. L. Harden, F. Lequeux, and J. P. Munch, *Phys. Rev. E* **67**, 031405 (2003).  
 [12] L. Cipelletti *et al.*, *Faraday Discuss.* **123**, 237 (2003).  
 [13] A. Duri and L. Cipelletti, *Europhys. Lett.* **76**, 972 (2006).  
 [14] J.-P. Bouchaud and E. Pitard, *Eur. Phys. J. E* **6**, 231 (2001).  
 [15] E. Zaccarelli *et al.*, *J. Chem. Phys.* **124**, 124908 (2006).  
 [16] A. Moussaïd *et al.* (unpublished).  
 [17] M. Sutton, K. Laaziri, F. Livet, and F. Bley, *Opt. Express* **11**, 2268 (2003).  
 [18] D. Lumma, L. B. Lurio, S. G. J. Mochrie, and M. Sutton, *Rev. Sci. Instrum.* **71**, 3274 (2000).  
 [19] R. Bandyopadhyay *et al.*, *Phys. Rev. Lett.* **93**, 228302 (2004).  
 [20] R. Aravinda Narayanan, P. Thiagarajan, S. Lewis, A. Bansal, L. S. Schadler, and L. B. Lurio, *Phys. Rev. Lett.* **97**, 075505 (2006).  
 [21] A. Robert *et al.*, *Europhys. Lett.* **75**, 764 (2006).  
 [22] A. Roshi, S. Barjami, G. S. Iannacchione, D. Paterson, and I. McNulty, *Phys. Rev. E* **74**, 031404 (2006).  
 [23] B. Chung *et al.*, *Phys. Rev. Lett.* **96**, 228301 (2006).  
 [24] P. Falus, M. A. Borthwick, S. Narayanan, A. R. Sandy, and S. G. J. Mochrie, *Phys. Rev. Lett.* **97**, 066102 (2006).  
 [25] L. Cipelletti, S. Manley, R. C. Ball, and D. A. Weitz, *Phys. Rev. Lett.* **84**, 2275 (2000).  
 [26] M. J. Solomon and P. Varadan, *Phys. Rev. E* **63**, 051402 (2001).